Excited Li and Na in He(n): influence of the dimer potential energy curves.

David Dell'Angelo, Grégoire Guillon, Alexandra Viel

Excited Li and Na in Hen: Influence of the dimer potential energy curves

David Dell'Angelo, Grégoire Guillon, and Alexandra Viel

Citation: J. Chem. Phys. **136**, 114308 (2012); doi: 10.1063/1.3693766
View online: http://dx.doi.org/10.1063/1.3693766
View Table of Contents: http://jcp.aip.org/resource/1/JCPSA6/v136/i11
Published by the American Institute of Physics.

Excited Li and Na in He_n: Influence of the dimer potential energy curves

David Dell'Angelo, Grégoire Guillon,[a] and Alexandra Viel
Institut de Physique de Rennes, UMR 6251, CNRS & Université de Rennes 1, F-35042 Rennes, France

(Received 24 November 2011; accepted 26 February 2012; published online 19 March 2012)

The $X^2\Sigma$ ground and the $A^2\Pi$ and $B^2\Sigma$ first two excited states of Li-He and Na-He are determined using high level complete active space self-consistent field-multireference configuration interaction *ab initio* method. The obtained potentials differ from the ones proposed by Pascale [Phys. Rev. A **28**, 632 (1983)], more strongly for the ground than for the excited states. Quantum diffusion Monte Carlo studies of small Li^*He_n and Na^*He_n with $n \leq 5$ are performed using a diatomics-in-molecule approach to model the non-pair additive interaction potential. The sensitivity of our results to the $A^2\Pi$ and $B^2\Sigma$ potentials used is assessed by an analysis of the structure and of the energetics of the clusters. For these small clusters, the physical conclusions are essentially independent of the diatomic curves employed. © *2012 American Institute of Physics*. [http://dx.doi.org/10.1063/1.3693766]

I. INTRODUCTION

The last two decades, helium clusters[1–3] have received considerable attention by many experimental and theoretical groups. These finite systems present unique and peculiar properties, like, for example, superfluidity. Various dopants, from atoms to large biological molecules, have been used to probe at the molecular scale, the interior and the surface properties of these liquid droplets. Helium nano-droplets also offer a quite unique weakly perturbing, cold, quantum in nature, superfluid environment with high thermal conductivity, ideal for the spectroscopy of diverse species including unstable and transient systems. In this perspective, the helium nanodroplet isolation spectroscopy[4–6] and its combination with electronic spectroscopy[7] is an advantageous alternative to cryogenic matrix isolation spectroscopy in the crystalline phase.

Alkali atoms appear to be among the best candidates for the study of electronic excitation due to the simple electronic configuration and the presence of optically accessible electronic transitions. In their electronic ground state, they reside on the helium cluster surface because the alkali-helium interaction is several times weaker than the helium-helium van der Waals attraction.[8,9] The electronic spectra of Li and of Na adsorbed at the surface of helium clusters have been recorded by numerous groups.[9–19] The most recent works[18,19] have probed highly excited (Rydberg) states of the dopant, Na in this case, whereas previous works focused on the two less energetic transitions associated to the D_1 and D_2 lines. The Li^*He and Na^*He exciplex formation after excitation of adsorbed Li and Na on helium clusters has been experimentally studied.[11,20,21] Spectroscopic data of this two light alkali in solid[22] and gaseous[23] helium have also been recorded. To the best of our knowledge, no laser-induced fluorescence spectra of Li and Na in liquid helium have been observed so far.[24] Theoretical works based on a combination of Monte Carlo and quantum mechanics calculations,[25] on the symmetry adapted cluster-configuration approach,[26] and on the relativistic density functional theory method[27] have proposed possible explanations for the difficulty of observing Li and Na spectra experimentally, which makes them peculiar among the alkali atoms.

In the large amount of theoretical papers focusing on alkali in helium droplets, a few address explicitly Li and Na in electronically excited states. Reho *et al.*[21] applied a one-dimensional model, quite successful to improve the understanding of the time dependence of NaHe exciplex formation. Pacheco *et al.*[28] used a quantum-classical model to describe Li attached to He_{99}. The absorption spectra as well as a method for the determination of highly excited state interaction potentials have recently appeared.[17,29]

Li^*He_p and Na^*He_p exciplexes with the alkali atom in the first excited state, consist of a ring of helium atoms located at the waist of the alkali atom p orbital. Different theoretical approaches predict different numbers of helium atoms in the ring. For Na, Dupont-Roc[30] found from five to six helium in the ring, Kanorsky *et al.*[31] five, while De-Toffol *et. al.*[32] estimated at least eight helium atoms. Quantum Monte Carlo studies of K^*He_n (Ref. 33) and of Rb^*He_n (Refs. 34 and 35) led to rings formed by six or seven, and seven helium atoms for K and Rb, respectively.

Pascale has provided in the early eighties[36,37] an extensive set of alkali-helium diatomic interaction potentials for ground and excited electronic states. More recent works[38,39] proposed alternative Rb-He interaction potentials and raised some criticism on the accuracy of Pascale's curves. Nevertheless, numerous theoretical conclusions have been drawn using models based on Pascale's diatomic energies. In particular, one of the authors studied the first and second excited states of small Rb-doped helium clusters, predicting a configuration with a ring of seven helium atoms for the first electronic state and a He-Rb-He core floating on a He_{n-2} cluster for the second excited state. However, in these works,[34,35] the dependence of the results on the diatomic curves used has not been tested.

The paper is organized as follows. The *ab initio* determination of LiHe and NaHe diatomic interactions as well as the model used for the interaction potential of the full cluster

[a]Present address: Department of Chemistry, University of Waterloo, Waterloo, Ontario N2L 3G1, Canada.

are described in Sec. II along with the technical details of the quantum Monte Carlo calculations. Detailed analyses of Li^*He_n and Na^*He_n energetics and structural properties at the classical and quantum levels are presented in Sec. III. Section IV concludes this work.

II. DESCRIPTION OF Ak^*-He_n SYSTEMS

A. Analytical potential energy surfaces for Ak^*He_n

A proper description of a global surface for systems such as Ak^*He_n is quite difficult for $n > 2$. In fact, not only the determination of energies by *ab initio* methods becomes rapidly prohibitive as n increases but even the representation of an analytical global surface in many dimensions is a non-trivial task. Schemes like the Shepard interpolation[40] provide global surfaces for large systems. However, in the case of Ak^*He_n, calculations of the *ab initio* energies required for such an interpolation scheme are out of reach given the current computer power. Approximations must thus be used. While in the case of dopants in the ground electronic state the usual pair approximation is physically appropriate, this is no longer the case for alkali atoms in the ^{2}P excited state. In our previous work,[34,35] the diatomics-in-molecule (DIM) (Ref. 41) approach that allows the proper modeling of the anisotropic Ak^*He interaction has been used. The representation of this anisotropic Ak^*He interaction is done[42] assuming that the relevant electronic configurations for Li^* and Na^* are purely [He]2p and [Ne]3p. Given the energy separation to other electronic excitations of Li and Na, no attempt of diabatization of the *ab initio* energies as proposed, for example, in Ref. 43 is done. The Russel-Saunders type spin-orbit coupling that becomes more and more important descending the period table can be included at the cost of doubling the size of the DIM matrix. Within this method, three global Ak^*He_n potential energy surfaces are obtained from the two first excited adiabatic Ak-He one-dimensional potential energy curves by diagonalization of a 6×6 complex matrix.

Beyond the obvious limitation of the accuracy of the representation of the global potential energy surfaces for Ak^*He_n made by using the DIM approach, the global surfaces obtained are related to the accuracy of the Ak^*-He curves on which the DIM matrix is built. However, due to the diagonalization step and to the dimensionality of the problem, establishing this relation is not trivial. In our previous works on rubidium atom,[34,35] we used consistently the curves of Pascale[36,37] despite the known criticisms about their accuracy.[38,39] We thus do not know if the conclusions of these works are strongly dependent on the quality of the Rb^*He curves employed.

B. Ak^*-He *ab initio* curves determination

A high level *ab initio* method, namely, complete active space self-consistent field-multireference configuration interaction (CASSCF-MRCI), is employed to obtain the interaction energy between a light alkali (Li or Na) atom and a He (^{1}S) atom. The small atomic number of these two alkalis allows scalar relativistic as well as spin-orbit effects to be neglected at this point. The $X^2\Sigma$ ground and the $A^2\Pi$ and $B^2\Sigma$ first two excited adiabatic states of Ak-He are obtained over a large range of intermolecular distances. MRCI calculations, using reference functions obtained from the state-averaged complete active space self-consistent field (SA-CASSCF) approach are chosen in order to get the highest possible accuracy on the excited states energies. The active space contains five σ-type and four π-type molecular orbitals. The former correlate asymptotically to the Li:2s,2p_0 (or Na:3s,3p_0) and He:1s,2s,2p_0 atomic orbitals, the latter to the Li:2p_1,2p_{-1} (or Na:3p_1,3p_{-1}) and He:2p_1,2p_{-1} atomic orbitals. All electrons are dynamically included in the calculations.

The uncontracted aug-cc-pV6Z basis set, formed using 186 primitive functions with contraction scheme (11s,6p,5d,4f,3g,2h) $\rightarrow$ [7s,6p,5d,4f,3g,2h] is used for the description of the helium atom. The use of such an extended basis set is expected to provide results for atomic and molecular properties very close to the complete basis set limit and to reduce dramatically the basis set superposition errors. On the other hand, improvements beyond the sextuple zeta basis set are likely to produce changes of similar magnitude as those expected from relativistic corrections or from breakdown of the Born-Oppenheimer approximation.[44] It thus appears that basis sets larger than cc-pV6Z are of little use within the realm of non-relativistic *ab initio* calculations. The total energy of the ground state of He is described very accurately using this aug-cc-pV6Z basis set, with the same −2.9034553532 Hartree value within ten digits for both CASSCF-MRCI and CCSD(T) methods. This computed energy is very close to the fairly accurate value of −2.903724375 Hartree obtained by Pekeris[45] with an explicitly correlated wave function as well as other very accurate and more recent calculations on He atom.[46–48] For Li, since a good description of the core is necessary, the aug-cc-pCVQZ basis set, containing additional tight functions, with contraction scheme (16s,10p,6d,4f,2g) $\rightarrow$ [9s,8p,6d,4f,2g] is employed. With this basis set, the energy difference between the ($1s^2 2s$) $^2S_0$ and ($1s^2 2p$) $^2P_0$, neglecting any spin-orbit coupling, is ΔE = 14 910.53 cm^{-1}, to be compared with 14 903.66 cm^{-1} and 14 904.00 cm^{-1} corresponding to the two D-lines, associated respectively with the $^2P_{1/2}$ and $^2P_{3/2}$ states of Li. For Na, the cc-pV5Z basis set which contains (23s,16p,8d,6f,4g,2h) Gaussian functions contracted into [11s,10p,8d,6f,4g,2h] is used. Allouche *et al.*[49] showed that the cc-pV5Z basis set yields accurate results, in particular for the well depth D_e and the minimum position R_e values for the $A^2\Pi$ state when compared with available experimental data.[50] Furthermore, only the inner 1s orbital of Na is treated as frozen in the CASSCF and MRCI calculations, leaving 11 electrons for which correlation effects are fully taken into account. The $^2S_0$ and $^2P_0$ levels are calculated to be 16 731.66 cm^{-1} apart. This value underestimates by about 235 cm^{-1} the experimental values for the sodium D-line transitions which are 16 956.17 cm^{-1} and 16 973.37 cm^{-1}, the spin-orbit coupling being 50 times bigger for Na than for Li. Although it is found to decrease the well depth of only a few tenth of a wavenumber, the counter-poise correction of Boys and Bernardi[51] is applied to the interaction energies between He and Ak in order to compensate for the basis set superposition errors.

A serious drawback of the (variational) MRCI method for calculating interaction energies resides in its lack of size-consistency, i.e., the computed energy for the Ak+He system at infinite separation R_∞ is not the sum of the separately computed energies of the isolated Ak and He moieties. This unlinked cluster effect can be accounted for by various corrections, losing, however, the variational behavior. The most popular Davidson-Silver correction[52,53] has been shown to overestimate the influence of the neglected quadruple excitations and hence total as well as complexation energies in a number of various situations[54–58] for which the Pople correction is more appropriate. Test calculations have shown that, in the case of Li-He and Na-He interactions, with the basis sets described above, the Davidson correction does not modify the complexation energies by more than 1%, although total energies are slightly lowered. Given the small magnitude of the correction and in order to stay consistent with previously published results[42] on alkali helium interactions, the more traditional Davidson correction has been used in this work. In addition, since the correction is only partial, the error quantity $\Delta E_{sc} = E_{AkHe}(R_\infty) - E_{Ak} - E_{He}$ with $R_\infty = 100\ a_0$ has been systematically subtracted from the pure complexation energy.

All the *ab initio* calculations are performed using the MOLPRO 2006.1 package.[59] In order to improve the accuracy of long-range interaction calculations, the thresholds for the neglect of one- and two-electron integrals on one hand, and those for the CASSCF, MRCI, and RCCSD(T) energy convergence, on the other hand, have been lowered to 10^{-13} and 10^{-9} Hartree, respectively.

C. Monte Carlo methods

The importance sampling diffusion Monte Carlo (IS-DMC) approach is used to obtain energies and structural properties of Ak^*He_n. DMC methods being described in numerous articles,[60–63] only technical details specific to the present work are given. As in our previous works[34,35] on Rb^* in He_n, the full Hamiltonian of the system contains the kinetic operator for the alkali and the n helium atoms, the He-He pair potential (Aziz HFD-B potential[64]) and the interaction between the helium atoms and the excited alkali atom described using the DIM approximation. Neglecting the electronic relaxation, we are left with the computation of the (node-less) vibrational ground state for which DMC is performant and exact. The lowest eigenvalue of the DIM matrix is used in this work. The stochastic resolution of the imaginary time Schrödinger equation implies the propagation of a finite size ensemble of walkers (points in the configuration space) using discretization of the imaginary time. The representation of the source term arising from the potential operator relies on a combination of weights carried by each walker and of a branching scheme. The scheme[65,66] as detailed in Ref. 67, results in a fixed ensemble size in which walkers with small weight are removed. At convergence of the walker distribution, the vibrational ground state energy can be computed from the average of the local energy or from the growth energy. The error bars are estimated via a blocking technique. The time propagation is splitted into blocks of n_{time} time steps, with n_{time} larger than the correlation length. The average over the ensemble is taken once per block from which the standard deviation is computed. The use of a discretized imaginary time as well as of a finite ensemble size results in bias that should be corrected. To this end, a double extrapolation to both zero time step and infinite ensemble size has been performed. The results are independent of the order of the two extrapolations performed. The error bars are estimated from the extrapolation procedures given the statistical error bars of each calculation.

TABLE I. Optimized parameters [in a.u.] of the trial wave function for Ak^*He_n clusters as defined in Eq. (1) and Eqs. (2).

	r_0	$a_{(HeHe)}$	$a_{(HeAk)}$
Li	16	500	50
Na	16	500	200

The product,

$$\Psi_T = \prod_{i\in He} \chi^{He}(r_{iA})\Phi^{HeAk}(r_{iA}) \prod_{i,j\in He} \Phi^{HeHe}(r_{ij}), \qquad (1)$$

is used for the trial function. Contrary to one used in Refs. 34 and 35, an explicit reference to the alkali atom is made in the trial function, Eq. (1), in which r_{iA} are the distances between the He atoms and the alkali atom, and r_{ij} the distances between two He atoms. The product in Eq. (1) contains Fermi-type and Jastrow-type functions,

$$\chi(r) = \{1 + \exp(r - r_0)\}^{-1}, \qquad (2a)$$

$$\Phi(r) = \exp(-ar^{-5}), \qquad (2b)$$

which are parameterized by r_0 and a given in Table I. The Jastrow-type functions avoid the sampling of too short helium-helium and alkali-helium distances for which the potential is strongly repulsive. The Fermi-type function confines the helium atoms inside a sphere centered at the alkali position, preferred location for the dopant in this first electronic state as shown for the Rb^*He_n system.[34]

After equilibration of the ensemble distribution, about 8000 blocks of 100 000 atomic unit of imaginary time using time step of 50 down to 10 a.u. have been performed. The ensemble size bias has been removed by extrapolation using various ensemble sizes up to 4000 walkers.

The density distributions are computed using a descendant-weighted scheme similar to the one described in Ref. 68. In the present work, a single accumulation step is used (cf., Eq. (15) of Ref. 68) and a relaxation time of 4000 a.u. has been found to provide converged results.

III. RESULTS

A. Classical analyses

The Li-He and Na-He ground $X\ ^2\Sigma$ and $A\ ^2\Pi$ excited curves are compared with the Patil[69] and the Cvetko[70] model valid for weakly interacting van der Waals systems and with the very accurate model of Kleinekathöfer, Tang, Toennies, and Yiu[71] (KTTY) based on the surface integral method.[72,73] For both systems, the well depths and the equilibrium

TABLE II. Comparison of well depths D_e [in cm^{-1}] and equilibrium distances R_e [in a_0] of the X $^2\Sigma$ and A $^2\Pi$ states of LiHe and NaHe.

	Li He				Na He			
	X $^2\Sigma$		A $^2\Pi$		X $^2\Sigma$		A $^2\Pi$	
	D_e	R_e	D_e	R_e	D_e	R_e	D_e	R_e
This work	−1.5	11.5	−1015	3.4	−1.2	12.4	−425	4.4
Pascale[a]	−2.5	11.2	−1020	3.5	−2.4	12.1	−500	4.5
Patil[b]	−1.3	11.7			−1.2	12.1		
Cvetko[c]	−1.4	11.5			−1.3	11.9		
KTTY[d]	−1.5	11.7			−1.3	12.2		
Mullamphy[e]			−980	3.4			−355	4.6
Hanssen[f]							−298.5	4.6
Nakayama[g]	−1.4	11.6	−1018	3.4	−1.2	12.2	−447	4.3

[a]Reference 36.
[b]Reference 69.
[c]Reference 70.
[d]Reference 71.
[e]Reference 74.
[f]Reference 75.
[g]Reference 42.

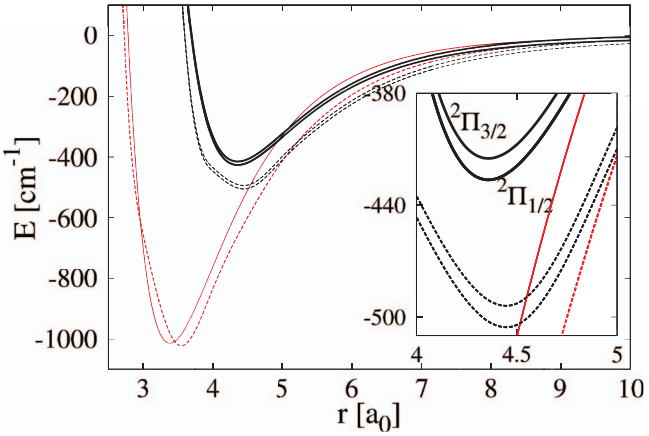

FIG. 1. $^2\Pi_{1/2}$ and $^2\Pi_{3/2}$ interaction curves for LiHe (red) and NaHe (black). The curves obtained from Pascale's potentials[36] (dashed lines) are compared with our *ab initio* curves (full line). A closer look of the region of the potential minima for NaHe is presented in the inset.

distances are reported in Table II, together with Pascale's values.[36] The consistent values of well depths and potential minimum positions we obtain when comparing with these models underline the correct choice of *ab initio* basis and level for these two systems. The table also shows a comparison of the A $^2\Pi$ excited state well depth D_e and minimum position R_e with the results of Hanssen *et al.*[75] and Mullamphy *et al.*[74] Reasonable agreement is obtained for the first excited state of both LiHe and NaHe systems. For the sake of completeness, the *ab initio* results by Nakayama *et al.*[42] obtained with basis sets smaller than the ones used here are presented in Table II. A fairly good agreement with these *ab initio* results for both the X $^2\Sigma$ and the A $^2\Pi$ can be remarked.

The difference with Pascale curves is in general more pronounced for both ground and excited states. Whereas significant differences are obtained for the ground state, the absolute values of the well depth for the A $^2\Pi$ states, more than two orders of magnitude deeper than the ground electronic state, make the relative difference between our potential curves and the one of Pascale less striking. For the A $^2\Pi$ state of LiHe, Pascale's, Nakayama's[42] and our value for the well depth agree with the experimental value of 1020 cm^{-1} reported by Lee *et al.*[76] to within 5 cm^{-1}. The difference observed for the A $^2\Pi$ state of NaHe is larger with a well depth of 425 cm^{-1} that is 15% shallower than in Pascale's curve. For both Li and Na, the B $^2\Sigma$ states are purely repulsive thus making comparisons with published data less straightforward. However when comparing with Pascale's curves, we find for both alkali curves that are less repulsive at short distances. For example, an excitation of 100 cm^{-1} above the asymptotic value is reached at 9.7 a_0 for LiHe (10.9 a_0 for NaHe) within our *ab initio* calculations while with Pascale's curves, this excitation is reached at 10.3 a_0 for LiHe (11.5 a_0 for NaHe). The representations of Li^*He_n and of Na^*He_n rely of both A $^2\Pi$ and B $^2\Sigma$ mixed within the DIM approach. The grasp of the effect of the differences obtained for the A $^2\Pi$ and B $^2\Sigma$ curves, still small, is however not trivial in the many-body case.

For the smallest LiHe and NaHe dimers, the first excited potential curves calculated including the spin orbit interaction are presented in Fig. 1. For the two considered alkali atoms, the $^2\Pi_{1/2}$ and $^2\Pi_{3/2}$ interaction curves computed either with Pascale's potentials[36] or with our *ab initio* curves are presented. The very small value of the Li spin orbit term, $\Delta_{SO} = 0.34$ cm^{-1}, induces a degeneracy splitting not visible on the energy scale of the figure. The larger effect of the Na spin orbit term, $\Delta_{SO} = 17.196$ cm^{-1}, is shown in the inset of the figure. Note that the $^2\Pi_{1/2}$ is lower in energy than the $^2\Pi_{3/2}$ state. As remarked above, the biggest difference observed in the LiHe potential curves is the minimum position. In addition, the figure shows that the curvature of the curves obtained with Pascale's potentials are smaller than the one obtained with our *ab initio* potentials. The differences observed for Na are more stringent. In addition to the shallower curves we obtain, as for Li the curvature of Pascale's curves is less pronounced than ours. The analysis of Fig. 1 gives a limited insight of the differences between the final multidimensional potential energy surfaces, in particular because of the diagonalization step of the DIM matrix.

Figure 2 presents two two-dimensional cuts of the $LiHe_2$ and $NaHe_2$ first excited surface, loosely referred to $^2\Pi_{1/2}$, retaining the diatomic notation. One alkali-helium distance is fixed such that the presented cuts contain the global minimum. For LiHe, such a distance is of 3.55 a_0 for Pascale's and 3.39 a_0 for our *ab initio* curves. Corresponding values for NaHe are 4.45 and 4.36 a_0, respectively. The position of the other helium atom is given in terms of the He $\widehat{Ak}$ He angle and of the distance to the alkali atom. For both systems the global potential minimum is obtained at a bent geometry, irrespective of the diatomic potentials used in the DIM matrix. In agreement with the analysis of the diatomic curves, the global minimum is lower in energy when Pascale's curves are used, in particular in the sodium case. Along this cut, the energy required to reach a linear configuration is systematically lower for our than for Pascale's diatomic potentials. This energy is

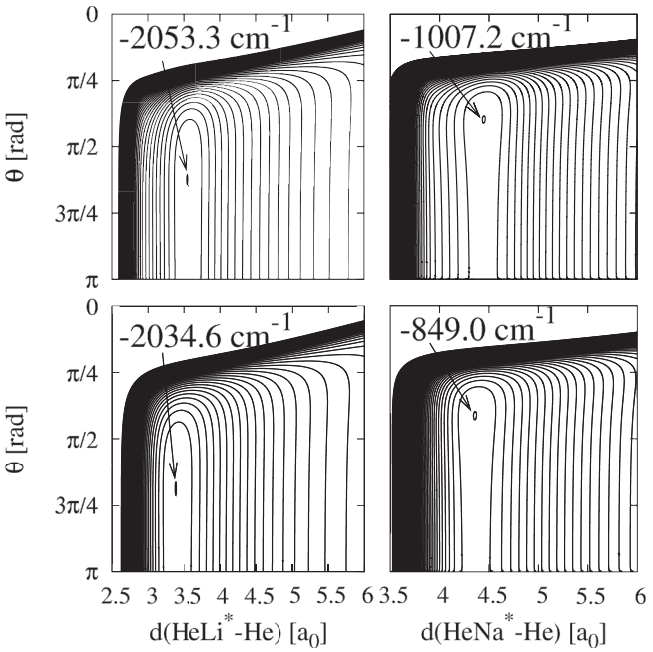

FIG. 2. Cuts of the first excited potential energy surface for Li^*He_2 (left) and Na^*He_2 (right) using Pascale's[36] (top) or the present interaction curves in the DIM matrix. The fixed alkali helium distance is such that the global minimum of potential indicated by the arrow is seen. θ corresponds to the He $\widehat{Ak}$ He angle while the abscissae is the distance between the alkali atom and the second helium atom. The contour lines are 50 cm^{-1} apart for the Li^*He_2 (left) system and 15 cm^{-1} for Na^*He_2 (right).

of about 4.4 cm^{-1} for $LiHe_2$ and of 1.1 cm^{-1} for $NaHe_2$ when using Pascale's diatomic curves, and 3.5 cm^{-1} for $LiHe_2$ and of 1 cm^{-1} for $NaHe_2$ when using our *ab initio* data.

Comparison of multidimensional surfaces is quite tedious. In the case of excited alkali atoms surrounded by n helium atoms, the particular geometries corresponding to regular rings of helium centered at the alkali atom have been shown to be of particular interest for better understanding the spectroscopy of alkali in liquid and solid helium.[8,30–32,77] These geometries correspond to all He $\widehat{Ak}$ He angles equal

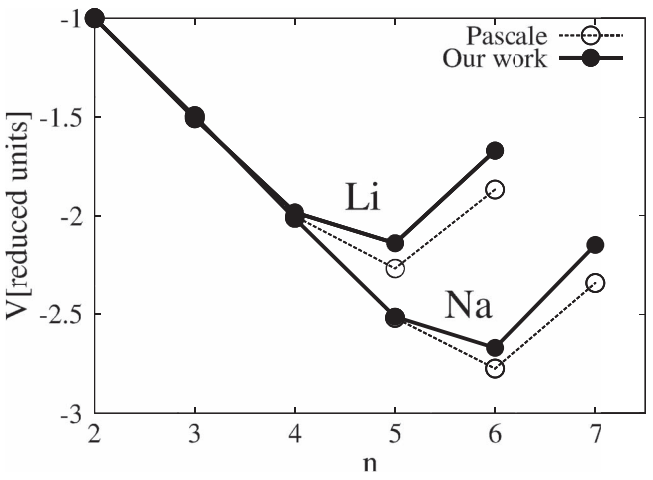

FIG. 3. Minimum of the potential energy surface within the regular ring constraint as a function of number of helium atoms, n, when our *ab initio* (filled circles) and Pascale's (open circles) diatomic curves are used in the DIM matrix. Values are rescaled with respect to the $n = 2$ value.

TABLE III. Vibrational ground state energies and chemical potential [in cm^{-1}] of $LiHe_n$ using our *ab initio* curves (a) and Pascale's (Ref. 36) curves (b) in the DIM matrix.

n	$E^{(a)}$	$-\mu^{(a)}$	$E^{(b)}$	$-\mu^{(b)}$
1	− 845.737 ± 0.001	845.50	− 862.033 ± 0.002	861.80
2	−1693.112 ± 0.002	847.38	−1725.641 ± 0.007	863.61
3	−2382.21 ± 0.04	689.10	−2430.69 ± 0.02	705.05
4	−2986.43 ± 0.05	604.22	−3081.51 ± 0.02	650.82
5	−3021.65 ± 0.05	35.22	−3259.16 ± 0.02	177.65

to $2\pi/n$ and to identical Ak-He distances. Figure 3 compares the evolution of the potential minimum as a function of n for these particular geometries. In order to ease the comparison, the minimum values have been rescaled by the absolute value of the $n = 2$ cluster for both alkali and both diatomic curves. Irrespective of the diatomic curves used in the DIM matrix, a linear variation is observed for $n \leq 4$ and $n \leq 5$ for Li and Na, respectively. The curves reach a minimum at the same n value, 5 for Li and 6 for Na. The relative values obtained for $LiHe_5$ and $NaHe_6$ are smaller when using Pascale's curves than when using our *ab initio* curves. The reason seems to stem from the occurrence of the potential minimum, within the ring geometry constraint, at larger alkali-helium distances in the former case, leading thus to a smaller He-He repulsion.

Root mean square calculations provide grasp of differences between multidimensional surfaces. These seem faithful for systems in which the minimum of potential plays a significant role in the vibrational ground state. However, for particular systems such as Ne^+He_n (Ref. 78) or Rb^*He_n,[34] it was shown that the vibrational ground state functions have little or even no amplitude in regions corresponding to the classical minimum of the potential surface. We thus refrain ourselves from computing such quantities.

B. Quantum results

Given the importance of zero point energy effects in helium clusters, the validity of the conclusions drawn from the analysis of the interaction potential surfaces must be ascertained when vibrational motion is included. The ground vibrational state energies computed using IS-DMC are presented in Table III for $LiHe_n$ and Table IV for $NaHe_n$ with n up to 5 for the two potential surfaces. In addition to the ground state energies, the chemical potential $\mu(n) = E(n) - E(n-1)$ is also provided. This quantity represents the binding energy for the nth helium. $\mu(1)$ is computed taking into account

TABLE IV. Same as in Table III for the $NaHe_n$ clusters.

n	$E^{(a)}$	$-\mu^{(a)}$	$E^{(b)}$	$-\mu^{(b)}$
1	− 344.257 ± 0.002	332.79	− 428.593 ± 0.003	417.13
2	− 677.972 ± 0.004	333.72	− 846.675 ± 0.003	418.08
3	− 954.534 ± 0.005	276.56	−1201.452 ± 0.004	354.78
4	−1227.64 ± 0.05	273.11	−1552.63 ± 0.01	351.18
5	−1432.02 ± 0.05	204.36	−1829.42 ± 0.03	276.79

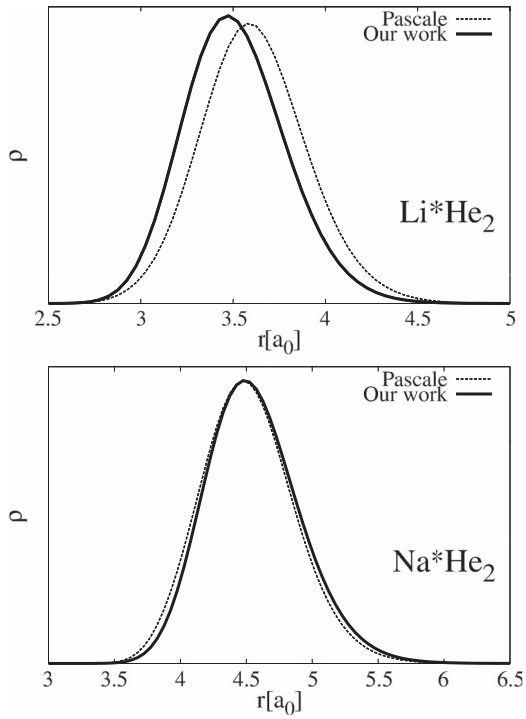

FIG. 4. Ak-He radial density distributions for $LiHe_2$ (top) and $NaHe_2$ (bottom) as a function of the Ak-He distance in a_0. The DIM surface used is based on our *ab initio* (full lines) or on Pascale's (dashed lines) diatomic interactions.

the spin orbit coupling of the bare alkali atoms. Calculations have been performed for the first solvation shell that contains up to $n = 5$ helium atoms. In the Na case, this number corresponds to one less helium atom than it can be supported by the surface, as can be seen on Fig. 3. This one helium atom difference due to the vibrational motion is also observed in $RbHe_n$ system,[34] and is due to the large zero point motion of the light helium atoms. The surfaces obtained using our *ab initio* data give both ground state energies and chemical potentials systematically larger than when using Pascale's curves. This means that the clusters are less bound in the former case as expected from the comparison of the diatomic curves. The largest difference occurs for $LiHe_5$. The calculations performed with our *ab initio* curves show that it is quite easy to remove the fifth helium atom with a chemical potential of $-35.22\ cm^{-1}$ only, five times less than the value of $-177.65\ cm^{-1}$ obtained with the surface based one Pascale's curves.

A more detailed comparison of the influence of the two surfaces can be carried out by looking at helium densities. The alkali helium radial densities obtained using the two potential surfaces are shown in Fig. 4 for $LiHe_2$ and $NaHe_2$. The Li-He distribution is shifted to larger distances when using our *ab initio* curves. This is consistent with the larger value of R_e for the $A^2\Pi$ state given in Table II. For $NaHe_2$, the two radial distributions are very similar. We infer that the stronger anharmonicity of the Pascale's diatomic curves (see Fig. 1) compensates the smaller R_e value. The same trend is observed when looking at the radial and at the angular distributions for $LiHe_5$ and $NaHe_5$ presented in Fig. 5. For these larger clusters, the use of either surface leads to virtually indistinguishable densities in the case of a dopant sodium atom. On the other hand, the $LiHe_5$ densities do present some differences. In particular, the angular $He\widehat{Ak}He$ distribution, consistent with a regular ring of 5 helium atoms, shows that the Li^*He_5 cluster obtained when using Pascale's rather than our

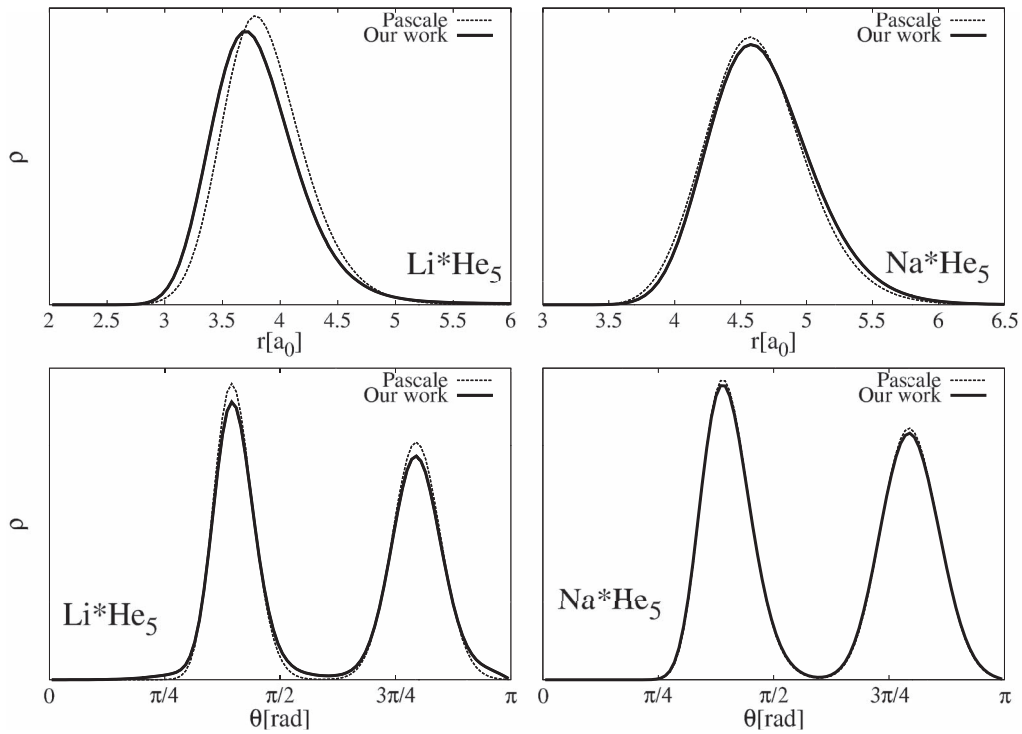

FIG. 5. Radial (top) and angular (bottom) distributions for $LiHe_5$ (left) and $NaHe_5$ (right). The DIM surface used is based on our *ab initio* (full lines) or on Pascale's (dashed lines) diatomic interactions.

curves is more rigid. Indeed the minimum of the distribution between the two maxima is closer to zero in this case.

IV. CONCLUSION

In this work, the $X^2\Sigma$ ground and the $A^2\Pi$ and $B^2\Sigma$ excited potential energies of LiHe and NaHe have been computed using the CASSCF-MRCI *ab initio* method. Convergence of the *ab initio* energies has been checked by comparison with published works, especially for the ground state. With the aim of studying Li^*He_n and Na^*He_n clusters, a systematic study of two global potential energy surfaces based on a DIM modeling and including the spin orbit coupling term has been performed. The surfaces differ by the $A^2\Pi$ and $B^2\Sigma$ diatomic energies used for building the DIM matrix, either Pascale's or our *ab initio* curves. In addition to the smaller well depths obtained with our *ab initio* curves, more subtle effects induced by the non-pair additive model used are obtained. The classical analysis is extended by IS-DMC computations of energetics and structural properties of Li^*He_n and Na^*He_n clusters in the first electronic excited state and with $n \leq 5$. Globally, the results are independent of the diatomic curves used, since in both cases clusters are found stable with up to 5 helium atoms in the first shell for Li and Na. The Li doped cluster helium densities show a stronger dependence on the diatomic curves used than the Na doped clusters. Concerning energetics, the largest difference is obtained for the chemical potential of $LiHe_5$ cluster. One can easily imagine that a larger difference in the diatomic curves could have led to a more marked difference in the clusters, like for example, pushing this fifth helium atom in the second solvation shell. In this work we stop the extensive comparison of the effect of the two global potential energy surfaces at clusters with five helium atoms. For Li and Na, these five helium fill the first shell. The helium density analysis shows that they are organized as a ring around the excited alkali atom. These rings structures are not observed in the photoexcitation of alkali adsorbed on helium clusters but have been detected in solid helium for heavier alkali (see, for example, Refs. 79 and 80). A barrier in the interaction potential felt by the alkali atom at the surface of He_n after electronic excitation is introduced to explain the non-observation of the ring structures in the droplet experiments.[21,34] Given the fact that the structures and energetics of the first shell do not strongly depend on the global surface used, a systematic comparison for larger clusters seems superfluous. Keeping in mind that the current study does not test the validity of the DIM approach used to represent the interaction potential, the physical conclusions obtained with Pascale's curves seem quite reasonable. A systematic study of the alkali series including larger cluster sizes using these curves is in progress.[81] Similar to Rb^*He_n, the inner ring structures perdure when the next solvation shell is built.[34] For much larger clusters, the details of how the coupling between the intra-ring modes and the collective excitations of the droplet could however strongly depend on the global surface used. Indeed the two Li^*He_5 chemical potentials suggest large differences in the ro-vibrational spectrum.

ACKNOWLEDGMENTS

This work is supported by the Région Bretagne via the project CREATE "4023-HELIUM," and via the project ANR "DYNHELIUM." We thank R. E. Zillich for interesting discussions.

[1] J. P. Toennies and A. F. Vilesov, Angew. Chem., Int. Ed. **43**, 2622 (2004).
[2] M. Barranco, R. Guardiola, S. Hernandez, R. Mayol, J. Navarro, and M. Pi, J. Low Temp. Phys. **142**, 1 (2006).
[3] F. Stienkemeier and K. K. Lehmann, J. Phys. B **39**, R127 (2006).
[4] J. P. Toennies and A. F. Vilesov, Annu. Rev. Phys. Chem. **49**, 1 (1998).
[5] K. K. Lehmann and G. Scoles, Science **279**, 2065 (1998).
[6] J. P. Toennies, A. F. Vilesov, and K. B. Whaley, Phys. Today **54**(2), 31 (2001).
[7] F. Stienkemeier and A. F. Vilesov, J. Chem. Phys. **115**, 10119 (2001).
[8] F. Ancilotto, E. Cheng, M. W. Cole, and F. Toigo, Z. Phys. B **98**, 323 (1995).
[9] F. Stienkemeier, J. Higgins, C. Callegari, S. I. Kanorsky, W. E. Ernst, and G. Scoles, Z. Phys. D **38**, 253 (1996).
[10] F. Stienkemeier, W. Ernst, J. Higgins, and G. Scoles, Z. Phys. B **98**, 413 (1995).
[11] J. Reho, C. Callegari, J. Higgins, W. E. Ernst, K. K. Lehmann, and G. Scoles, Faraday Discuss. **108**, 161 (1997).
[12] C. Callegari, J. Higgins, F. Stienkemeier, and G. Scoles, J. Phys. Chem. A **102**, 95 (1998).
[13] F. Stienkemeier, M. Wewer, F. Meier, and H. Lut, Rev. Sci. Instrum. **71**, 3480 (2000).
[14] F. Stienkemeier, O. Bünermann, R. Mayol, F. Ancilotto, and M. Barranco, Phys. Rev. B **70**, 214509 (2004).
[15] R. Mayol, F. Ancilotto, M. Barranco, O. Bünermann, M. Pi, and F. Stienkemeier, J. Low Temp. Phys. **138**, 229 (2005).
[16] O. Bünermann, G. Droppelmann, A. Hernando, R. Mayol, and F. Stienkemeier, J. Phys. Chem. A **111**, 12684 (2007).
[17] A. Hernando, M. Barranco, R. Mayol, M. Pi, F. Ancilotto, O. Bünermann, and F. Stienkemeier, J. Low Temp. Phys. **158**, 105 (2010).
[18] E. Loginov and M. Drabbels, Phys. Rev. Lett. **106**, 083401 (2011).
[19] E. Loginov, C. Callegari, F. Ancilotto, and M. Drabbels, J. Phys. Chem. A **115**, 6779 (2011).
[20] J. Reho, J. Higgins, C. Callegari, K. K. Lehmann, and G. Scoles, J. Chem. Phys. **113**, 9686 (2000).
[21] J. Reho, J. Higgins, K. K. Lehmann, and G. Scoles, J. Chem. Phys. **113**, 9694 (2000).
[22] P. Moroshkin, A. Hofer, and A. Weis, Phys. Rep. **469**, 1 (2008).
[23] K. Enomoto, K. Hirano, M. Kumakura, Y. Takahashi, and T. Yabuzaki, Phys. Rev. A **69**, 012501 (2004).
[24] Y. Takahashi, K. Sano, T. Kinoshita, and T. Yabuzaki, Phys. Rev. Lett. **71**, 1035 (1993).
[25] V. Ludwig, P. K. Mukherjee, K. Coutinho, and S. Canuto, Phys. Rev. A **72**, 062714 (2005).
[26] B. Saha, R. Fukuda, H. Nakatsuji, and P. K. Mukherjee, Theor. Chem. Acc. **118**, 437 (2011).
[27] J. Anton, P. K. Mukherjee, B. Fricke, and S. Fritzsche, J. Phys. B **40**, 2453 (2011).
[28] A. B. Pacheco, B. Thorndyke, A. Reyes, and D. A. Micha, J. Chem. Phys. **127**, 244504 (2007).
[29] C. Callegari and F. Ancilotto, J. Phys. Chem. A **115**, 6789 (2011).
[30] J. Dupont-Roc, Z. Phys. B **98**, 383 (1995).
[31] S. Kanorsky, A. Weiss, M. Arndt, R. Dziewior, and T. W. Hänsch, Z. Phys. B **98**, 371 (1995).
[32] G. DeToffol, F. Ancilotto, and F. Toigo, J. Low Temp. Phys. **102**, 381 (1996).
[33] T. Takayanagi and M. Shiga, Phys. Chem. Chem. Phys. **6**, 3241 (2004).
[34] M. Leino, A. Viel, and R. E. Zillich, J. Chem. Phys. **129**, 184308 (2008).
[35] M. Leino, A. Viel, and R. E. Zillich, J. Chem. Phys. **134**, 024316 (2011).
[36] J. Pascale, Phys. Rev. A **28**, 632 (1983).
[37] J. Pascale, Technical Report, Service de Physique des Atomes et des Surfaces (C.E.N. Saclay), Gif sur Yvette, France, 1983.
[38] K. Hirano, K. Enomoto, M. Kumakura, Y. Takahashi, and T. Yabuzaki, Phys. Rev. A **68**, 012722 (2003).
[39] M. Mudrich, F. Stienkemeier, G. Droppelmann, P. Claas, and C. P. Schulz, Phys. Rev. Lett. **100**, 023401 (2008).
[40] J. Ischtwan and M. A. Collins, J. Chem. Phys. **100**, 8080 (1994).

[41]F. O. Ellison, J. Am. Chem. Soc. **85**, 3540 (1963).
[42]A. Nakayama and K. Yamashita, J. Chem. Phys. **114**, 780 (2001).
[43]M. C. Heitz, L. Teixidor, N. T. Van-Oanh, and F. Spiegelman, J. Phys. Chem. A **114**, 3287 (2010).
[44]U. Kleinekathöfer, M. Lewerenz, and M. Mladenović, Phys. Rev. Lett. **83**, 4717 (1999).
[45]C. L. Pekeris, Phys. Rep. **115**, 1216 (1959).
[46]M. I. Haftel and V. B. Mandelzweig, Phys. Rev. A **38**, 5995 (1988).
[47]J. D. Baker, D. E. Freund, R. N. Hill, and J. D. Morgan III, Phys. Rev. A **41**, 1247 (1990).
[48]M. Braun, W. Schweizer, and H. Herold, Phys. Rev. A **48**, 1916 (1993).
[49]A. R. Allouche, K. Alioua, M. Bouledroua, and M. Aubert-Frécon, Chem. Phys. **355**, 85 (2009).
[50]M. D. Havey, S. E. Frolking, and J. J. Wright, Phys. Rev. Lett. **45**, 1783 (1980).
[51]S. F. Boys and F. Bernardi, Mol. Phys. **19**, 553 (1970).
[52]S. R. Langhoff and E. R. Davidson, Int. J. Quantum Chem. **8**, 61 (1974).
[53]E. R. Davidson and D. W. Silver, Chem. Phys. Lett. **52**, 403 (1977).
[54]P. M. W. Gill, M. W. Wong, R. H. Nobes, and L. Radom, Chem. Phys. Lett. **148**, 541 (1988).
[55]L. Latifzadeha and K. Balasubramanian, Chem. Phys. Lett. **243**, 243 (1995).
[56]R. Siebert, P. Fleurat-Lessard, R. Schinke, M. Bittererová, and S. C. Farantos, J. Chem. Phys. **116**, 9749 (2002).
[57]D. P. Schofield and H. G. Kjaergaard, J. Chem. Phys. **120**, 6930 (2004).
[58]M. Honigmann, R. J. Buenker, and H. P. Liebermann, J. Chem. Phys. **120**, 034303 (2009).
[59]H.-J. Werner, P. J. Knowles, R. Lindh, F. R. Manby, M. Schütz *et al.*, MOLPRO, version 2006.1, a package of *ab initio* programs, 2006, see http://www.molpro.net.
[60]P. J. Reynolds, D. M. Ceperley, B. J. Alder, and W. A. Lester, J. Chem. Phys. **77**, 5593 (1982).
[61]M. A. Suhm and R. O. Watts, Phys. Rep. **204**, 293 (1991).
[62]C. J. Umrigar, M. P. Nightingale, and K. J. Runge, J. Chem. Phys. **99**, 2865 (1993).
[63]B. L. Hammond, W. A. Lester, and P. J. Reynolds, *Monte Carlo Methods in Ab Initio Quantum Chemistry* (World Scientific, Singapore, 1994).
[64]R. A. Aziz, F. R. W. McCourt, and C. C. K. Wong, Mol. Phys. **61**, 1487 (1987).
[65]M. Lewerenz, private communication (2006).
[66]D. Blume, M. Lewerenz, F. Huisken, and M. Kaloudis, J. Chem. Phys. **105**, 8666 (1996).
[67]A. Viel, M. D. Coutinho-Neto, and U. Manthe, J. Chem. Phys. **126**, 024308 (2007).
[68]J. Casulleras and J. Boronat, Phys. Rev. B **52**, 3654 (1995).
[69]S. H. Patil, J. Chem. Phys. **94**, 8089 (1991).
[70]D. Cvetko, A. Lausi, A. Morgante, F. Tommasini, P. Cortona, and M. G. Dondi, J. Chem. Phys. **100**, 2052 (1994).
[71]U. Kleinekathöfer, K. T. Tang, J. P. Toennies, and C. L. Yiu, Chem. Phys. Lett. **249**, 257 (1996).
[72]T. Holstein, J. Phys. Chem. **56**, 832 (1952).
[73]B. M. Smirnov and M. I. Chibisov, Sov. Phys. JETP **21**, 624 (1965).
[74]D. F. T. Mullamphy, G. Peach, V. V. I. B. Whittingham, and S. J. Gibson, J. Phys. B **40**, 1141 (2007).
[75]J. Hanssen, R. McCarroll, and P. Valiron, J. Phys. B **12**, 899 (1979).
[76]C. J. Lee, M. D. Havey, and R. P. Meyer, Phys. Rev. A **43**, 77 (1991).
[77]M. Beau, H. Günther, G. zu Putlitz, and B. Tabbert, Z. Phys. B **101**, 253 (1996).
[78]C. A. Brindle, M. R. Prado, K. C. Janda, N. Halberstadt, and M. Lewerenz, J. Chem. Phys. **123**, 064312 (2005).
[79]A. Hofer, P. Moroshkin, D. Nettels, S. Ulzega, and A. Weis, Phys. Rev. A **74**, 032509 (2006).
[80]P. Moroshkin, A. Hofer, V. Lebedev, and A. Weis, Phys. Rev. A **78**, 032501 (2008).
[81]D. Dell'Angelo and A. Viel, "Quantum study of helium clusters doped with electronically excited Li, Na, K, and Rb atoms" (unpublished).